

A model for space and time-like proton (neutron) form factors

E. A. Kuraev,¹ E. Tomasi-Gustafsson,^{2,*} and A. Dbeysi²

¹*Joint Institute for Nuclear Research, Dubna, Russia*

²*Univ Paris-Sud, CNRS/IN2P3, Institut de Physique Nucléaire, UMR 8608, 91405 Orsay, France*

(Dated: June 10, 2011)

Recent experiments on the electromagnetic proton and neutron form factors reveal very peculiar features such as the decreasing of the ratio of electric to magnetic form factor of the proton as function of the transfer momentum squared, in electron proton elastic scattering. A model is suggested to describe the known experimental behavior of nucleon form factors both in space and time-like regions. It implies quarks to be colorless in the region of high intensity chomo-magnetic gluon field inside the nucleon.

Measurements on the nucleon form factors (FFs) are traditionally based on the measurement of the unpolarized differential cross section in electron-proton elastic scattering. Recently the polarization transfer method [1] was applied by the GEP collaboration at Jlab. The experiments [2] show a definite indication of the decreasing the proton electric form factor when the momentum transfer squared $Q^2 = -q^2$ increases.

Future plans of precise measurements motivate the necessity of new models of the nucleon at large momentum transfer squared, which is able to explain the present data and to give predictions in space-like as well as in time-like region.

In the space-like region, in non relativistic approaches (and also in relativistic approaches, but only in the Breit frame) the electromagnetic nucleon FFs are defined as the Fourier transform of the charge and magnetic distributions inside the proton.

The purpose of this work is to give a qualitative understanding of the experimental finding of the fast decreasing of the charge distribution at small distances inside the proton. The same modelization should apply also to the neutron, and describe all existing data in space-like and time-like regions of the momentum transfer squared. The annihilation region is best described in center of mass (CMS) system of the proton-antiproton system (in initial or final state). Charged lepton-nucleon scattering (in space-like (SL) region) and the annihilation of a nucleon-antinucleon pair in electron-positron, or the production of lepton pairs in proton-antiproton annihilation (in time-like (TL) region) provide the possibility to investigate the charge distribution inside the proton. Our considerations hold in both regions, in Breit frame for space-like region and in CMS in time-like region, and will be derived as function of q^2 , which is invariant.

Let us consider the analogy with gravitation. Newton showed that for a spherical symmetric distributed mass density, a point located at a distance $R < R_0$ from the center (R_0 is the radius of the object) is submitted to a gravitational force due only to the matter located inside the surface where the point is located. The gravitational interaction with the layer of matter situated at $r > R$ is fully compensated and its effect vanishes. The Coulomb

force between the electron and the proton has a similar behavior as the gravitational potential. The Newton-like theorem mentioned above, works only for the scalar part ϕ of the electromagnetic field, $A = (\phi, \vec{A})$, not for the vector potential \vec{A} , which is related to the magnetic field. These arguments apply to the electric and magnetic proton form factors, and suggest that their ratio should be:

$$\mu G_E / G_M \simeq \left(\frac{1}{rQ} \right)^3, \quad Q > \frac{1}{r}. \quad (1)$$

For a value of $r \leq 0.7$ fm, one obtains $Q \geq 0.29$ GeV. Such behavior is not confirmed by the experimental data.

Let us consider the proton as a system consisting of three valence quark and of a neutral sea consisting of gluons and quark-antiquark pairs. It is usually assumed that the nucleon is an antisymmetric state of colored quarks

$$\begin{aligned} |p\rangle &\sim \epsilon_{ijk} |u^i u^j d^k\rangle, \\ |n\rangle &\sim \epsilon_{ijk} |u^i d^j d^k\rangle. \end{aligned} \quad (2)$$

The main idea of this work, is that the spatial center of the nucleon (proton and neutron) is electrically neutral, therefore this expectation must be drastically changed, starting at some value of Q or for distances smaller than some radius.

This representation fails inside the nucleon where the region of a strong gluonic field may create a gluonic condensate of clusters with randomly oriented chromo-magnetic field [3]. The strength of the gluon field in vacuum (G refers to the gluon field tensor $G_{\mu\nu}$) is

$$\langle 0 | \frac{\alpha_s}{\pi} (G_{\mu\nu}^a)^2 | 0 \rangle = 0.012 \text{ GeV}^4. \quad (3)$$

From this value, taking $\alpha_s/\pi \sim 0.1$, one can find that the strength of the chromo-electric field has the value:

$$G^2 \simeq \frac{\pi}{\alpha_s} 0.012 \text{ GeV}^4, \quad i.e., \quad E \simeq 0.245 \text{ GeV}^2. \quad (4)$$

At smaller distances the gluonic field as well as the number of gluons increase. Therefore, the strength of the chromo-electric field increases as well. Our main assumption consists in the statement that in the region

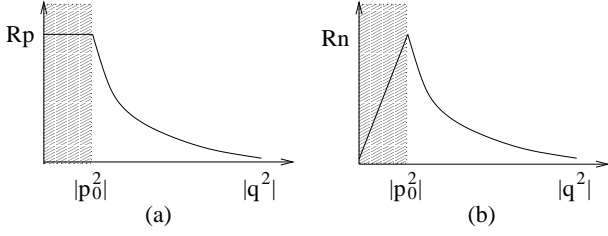


Figure 1. Schematic modelisation of ratio of the electric to magnetic proton (a) and neutron (b) FFs as a function of Q^2 . The shadowed area shows the region where the present model is not applicable.

of strong chromo-magnetic field the color quantum number of quarks does not play any role, due to stochastic averaging. Let us formalize this property in the following way:

$$\langle G|u^i u^j|G \rangle \sim \delta_{ij}. \quad (5)$$

For the neutron, the same property applies, where the u quark is replaced by the d quark. When the color quantum number of quarks of the same flavor vanishes, then, due to Pauli principle, uu (or dd) quarks are pushed outside the internal region of the proton (or the neutron). The third quark is attracted by one of the identical quarks and forms a compact diquark. In the regions of not so intense gluonic field the color state of quarks is restored. Let us estimate the distance (or transferred momentum) where it may happen. The creation of a quark-diquark dipole system occurs when the attraction force exceeds the stochastic force of the gluon field:

$$\frac{Q_q^2 e^2}{r_0^2} > eQ_q E. \quad (6)$$

where Q_q is the charge of the isolated quark (u (d) in case of proton(neutron) and r_0 is the distance between the quark and the diquark system. Taking into account the relation: $r_0 p_0 = 1$, one obtains

$$p_0 = \sqrt{\frac{E}{Q_q e}} = 1.1 \text{ GeV}. \quad (7)$$

The minimal distance where the quark-diquark picture appears is $r_0 = 0.22$ (0.31) fm in the proton (neutron), which corresponds to $p_0^2 = 1.21$ (2.43) GeV^2 . A qualitative and schematic picture of our model is illustrated in Fig. 1, where the ratio $R_{p,n}$ is shown as a function of q^2 in the space-like region. Quark counting rules apply to the vector part of the potential, and correspond to the interaction of virtual photon with three independent quarks. The corresponding behavior of FFs is [4, 5]:

$$\begin{aligned} G_M(Q^2) &= \mu_p G_E(Q^2); \\ G_E(Q^2) &= G_D(Q^2) = [1 + Q^2/(0.71 \text{ GeV}^2)]^{-2} \end{aligned} \quad (8)$$

where Q^2 is expressed in GeV^2 and FFs are normalized respectively as $G_E(0) = 1$, $G_M(0) = \mu_p$, (μ_p is the anomalous proton magnetic moment). The present model leaves unchanged the prediction for the magnetic FF. An additional suppression mechanism of the electric FF is provided by the 'central' region of the hadron (we consider now the scattering kinematics). An effect similar to the screening of a charge in plasma may take place. The scalar part of the electromagnetic field ϕ obey the equation:

$$\Delta\phi = -4\pi e \sum Z_i n_i, \quad n_i = n_{i0} \exp\left[-\frac{Z_i e \phi}{kT}\right] \quad (9)$$

where Z_i (n_i) are the charges (density) of current $q\bar{q}$ pairs in the zero charge region, T is the effective temperature of the hot plasma. Expanding the Boltzmann exponent and using the neutrality condition: $\sum Z_i n_{i0} = 0$ we obtain:

$$\Delta\phi - \chi^2 \phi = 0, \quad \phi = e^{-\frac{\chi r}{r}}. \quad (10)$$

The distribution to momentum space, obtained through the Fourier transform, shows that the central region provides an additional suppression for the electric FF:

$$G_E(Q^2) = G_M(Q^2) (1 + Q^2/q_1^2)^{-1} \quad (11)$$

where q_1 should be considered a fitting parameter, different in principle for proton and neutrons. This gives the following dependence for the form factor ratio, in SL region:

$$R_{p,n}(Q^2) = \frac{G_E(Q^2)}{G_M(Q^2)} \sim (q^2 + q_{1(p,n)}^2)^{-1}. \quad (12)$$

Let us precise this statement, considering now the annihilation channel, for example the process $e^+ + e^- \rightarrow \gamma^*(q) \rightarrow p + \bar{p}$. In the center of mass reference frame, the three-dimensional transferred momentum vanishes.

Let us generalize the definition of FFs in the following way:

$$F(q^2) = \int_{\mathcal{D}} d^4x e^{iq_\mu x^\mu} \rho(x), \quad q_\mu x^\mu = q_0 t - \vec{q} \cdot \vec{x} \quad (13)$$

where $\rho(x) = \rho(\vec{r}, t)$ is the space-time distribution of the electric charge in a space-time volume \mathcal{D} .

In the scattering channel, $e + p \rightarrow e + p$ and in the Breit frame, we recover the usual definition of FFs:

$$F(q^2) = \delta(q_0) F(Q^2), \quad Q^2 = -(q_0^2 - \vec{q}^2) > 0. \quad (14)$$

where the zero energy transfer is implied.

In the annihilation channel, we have:

$$F(q^2) = \int_{\mathcal{D}} dt e^{i\sqrt{q^2}t} \int d^3\vec{r} \rho(\vec{r}, t) = \int_{\mathcal{D}} dt e^{i\sqrt{q^2}t} Q(t), \quad (15)$$

where $\mathcal{Q}(t)$ describes the time evolution of the charge distribution in the domain \mathcal{D} .

We discuss now the mechanism of $\bar{p}p$ creation in e^+e^- annihilation through spin one intermediate state ${}^3S_1 = \langle 0|J^\mu|p\bar{p}\rangle$. We can describe this process in three steps.

1) Above the physical threshold, $q^2 \geq 4M^2$, the vacuum state transfers all the energy released by the electron-positron annihilation to a S-wave state with total spin 1 and four momentum $q = (\sqrt{q^2}, 0, 0, 0)$. This state of matter consists in at least six massless valence current quarks, a set of gluons and a sea of current $q\bar{q}$ current quarks, with total energy $q_0 > 2M_P$, and total orbital momentum unity. Such state, which is created in a small spatial volume of the order $h/\sqrt{q^2}$, starts to expand and cool down. The current quarks (antiquarks) absorb gluons and transform into constituent quarks (antiquarks).

2) The next step is the evolution of real (colorless) proton and antiproton creation, with the known size $h/(2M_p) \sim 0.1$ fm. The residual energy turns into kinetic energy of motion, with relative velocity $2\beta = 2\sqrt{1 - 4M_p^2/q_0^2}$. In the first stages, the strong chromo-electric (chromo-magnetic) field leads to an effective loss of color freedom of quarks and antiquarks. As a result of Fermi statistics, the identical (colorless) quarks (uu in the proton and dd in the neutron) are repulsed. The remaining quark (antiquark) of different flavor is attracted to one of the quarks at the surface, creating a compact diquark (du state).

3) In the last stage, the long range color forces create a stable colorless state of proton and antiproton. Part of the initial energy is dissipated into the transmission of current valence quarks and antiquarks to the constituent ones, which give origin to on-shell proton and antiproton. At this stage of evolution, the two sets of quarks and antiquarks are separated by a distance R . The repulsion of proton and antiproton which tend to move in opposite directions with kinetic energy $T = \sqrt{q^2} - 2M_p c^2$ is balanced by the confinement potential $q_0 - 2M c^2 = (k/2)R^2$. For extreme small values of the velocity $\alpha\pi/\beta \simeq 1$ the final state interaction leads to the formation of a $N\bar{N}$ bound state, with size of the order of 100 fm. At larger distances, the inertial force exceeds the confinement force proton and antiproton start moving, each one with velocity β . The spin unity of the intermediate virtual photon manifests itself in dynamical polarizations of proton and antiproton.

The complex nature of FFs in TL region arises naturally from final state interaction, being larger in the threshold region and vanishing at large q^2 . This is in agreement with the Phragmén-Lindelöf theorem [6], which applies to analytical functions of complex variables, and insures the equality of form factors for large values of $|q^2|$. As form factors are real in the scattering channel, it has for consequence that the imaginary part

must vanish in the annihilation channel at large $|q^2|$.

The present model is in agreement with the finding of Ref. [7] of a point-like nature of FFs at threshold. based on arguments on the absence of resummation of Coulomb corrections near threshold, the extraction of FFs from the experimental cross sections is consistent with $|G_E^2| = |G_M^2| = 1$. Therefore, the present model suggests the following parametrization in TL region ($q^2 > 4M_p^2$):

$$G_M(q^2) = \mu_p [1 + (q^2 - 4M_p^2)/q_1^2]^{-2} \quad (16)$$

$$G_E(q^2) = G_M(q^2) [1 + (q^2 - 4M_p^2)/q_1^2]^{-2}. \quad (17)$$

As for the magnetic FFs, it is defined by the distribution of the angular momentum (spin), similarly for proton and neutron. It is expected that proton and neutron magnetic FFs are similar and that are slowly varying functions of Q^2 , as determined by quark counting rules.

The world data on proton FFs together with the predictions of the model are shown in Fig. 2.

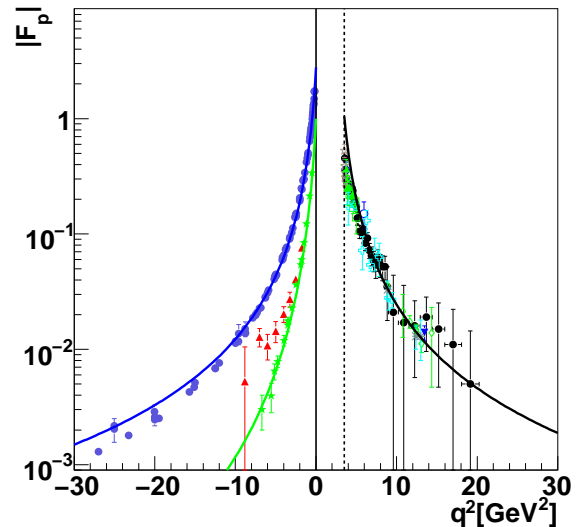


Figure 2. World data on proton FFs as function of q^2 . **Space-like region:** $G_M(Q^2)$ data (blue circles), dipole function (blue line) from Eq. (8); electric FF, $G_E(Q^2)$, from unpolarized measurements (red triangles) and from polarization measurements (green stars). The green line is the model prediction from Eq. (11). **Time-like region:** world data for $|G_E| = |G_M|$ (various symbols for $q^2 > 4M_p^2$ and model prediction (black line) from Eq. (16).

In the Space-like region, the magnetic FF, $G_M(Q^2)$ (blue circles) is well reproduced by the dipole function (8) (blue line) normalized to $G_M(0) = \mu_p$. The electric FF, $G_E(Q^2)$ from unpolarized measurements (red triangles) also follows a dipole function normalized to $G_E(0) = 1$. $GE(Q^2)$ (green stars) from polarized measurements is well reproduced by the prediction of the present model (green line), Eq. (11), setting $q_1^2 = 3.6$ GeV².

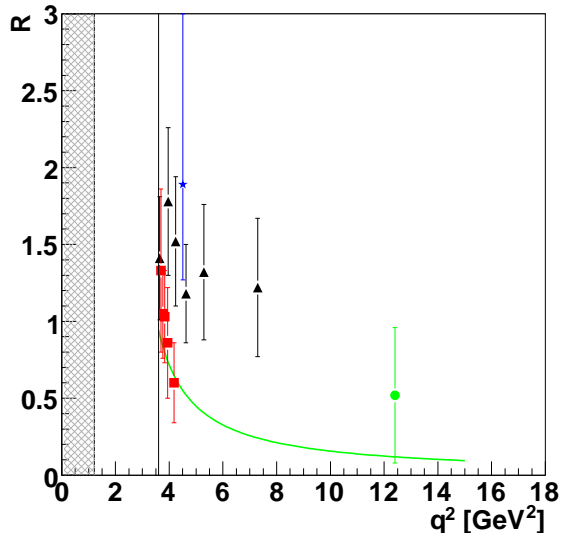


Figure 3. Proton electromagnetic FF ratio in TL region, as functions of $|q^2|$. The line is the prediction of the present model. Data are from Ref. [9] (red squares), from Ref. [8] (black triangles), from Ref. [10] (green circle), and from Ref. [11] (blue star).

In the time-like region, the individual determination of G_E and G_M has not been done, due to the lower luminosity achieved up to now. The experimental results, corresponding to the annihilation cross section, are given in terms of $|G_M|$, assuming $|G_E| = |G_M|$ or $|G_E| = 0$. The data for $|G_E(q^2)| = |G_M(q^2)|$ are shown for $q^2 > 4M_p^2$ in Fig. 2 (black circles) for various experiments, see Ref. [8] and are well reproduced by the present model, following Eq. (16) with $q_2^2 = 1.2 \text{ GeV}^2$ (black line).

The few existing data on the proton FF ratio in TL region are reported in Fig. 3: from [9] (red squares), from Ref. [8] (black triangles), from Ref. [10] (green circle), and from Ref. [11] (blue star). The prediction of the present model is drawn as a solid line. The line is normalized at the kinematical threshold, $q^2 = 4M_p^2$, where $|G_E(q^2)| = |G_M(q^2)|$ (assumed = 1). Due to the dispersion of the data, we do not try any fit, but we apply Eqs.(16, 17) with $q_1^2 = 1.2 \text{ GeV}^2$. Concerning the neutron, experimental data are more scarce, imprecise and extend to a smaller Q^2 range, due to the smallness of the electric FF. The neutron and proton electric FFs in SL region are shown in Fig 4. A sample of the existing neutron data is shown (black triangles) (see Ref. [12] and Refs therein). For comparison, the proton FF from polarization data [2] is shown (green, stars) and from Rosenbluth method [13] (red, triangles). The prediction is the solid, green line for the proton FF and the black, dashed line for the neutron following Eq. (8) with $q_1^2 = 2.42$. The vertical line indicates the region where the present model does not apply to the neutron.

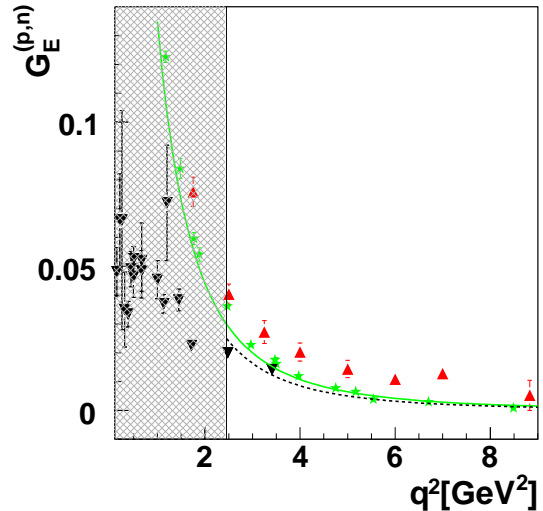


Figure 4. World data on neutron electric FF (black, triangle down), in SL region, as functions of $|q^2|$. For references on neutron experimental data see Ref. [12]. For comparison, the proton FF from polarization data [2] is shown (green, stars) and from Rosenbluth method [13] (red, triangles). The prediction is shown as a solid, green line for the proton FF and as a black, dashed line for the neutron. The normalization is arbitrary. The vertical line indicates the region where the present model does not apply (for the neutron).

In TL region few data exist, based on only one experiment [11], and they are shown in Fig. 5. The prediction (Eq.(16) with $q_{1,n}^2 = 1.2$) is shown as a solid, black line. The line is normalized at the kinematical threshold, $q^2 = 4M_p^2$, $|G_{En}(q^2)| = |G_{Mn}(q^2)|$ (assumed = 1). The solid line indicates the limit where the present model applies. The dashed line indicates the kinematical threshold. We do not try any fitting, as on one side the data are not very precise, and on the other side they have not been extracted with the point-like prescription at threshold, so that they partly include the Coulomb corrections. The comparison to TL data will be better done in future with the integrated cross section itself, instead that with the generalized FF.

In conclusion, we have developed an intuitive and qualitative model, which satisfies the known features of the data and the physical requirements. We have generalized the definition of FFs in all the kinematical range: the physical meaning of FFs in SL region is related to the charge and magnetic distributions in the (Breit system), whereas in TL region it is related to the time evolution of these distributions, as expressed in Eq. (13). The complex nature of FFs in TL region arises naturally from final state interaction, being larger in the threshold region and vanishing at large q^2 . This is in agreement with the Phragmén-Lindelöf theorem [6], which applies

clean FFs data, in space-like and time-like regions.

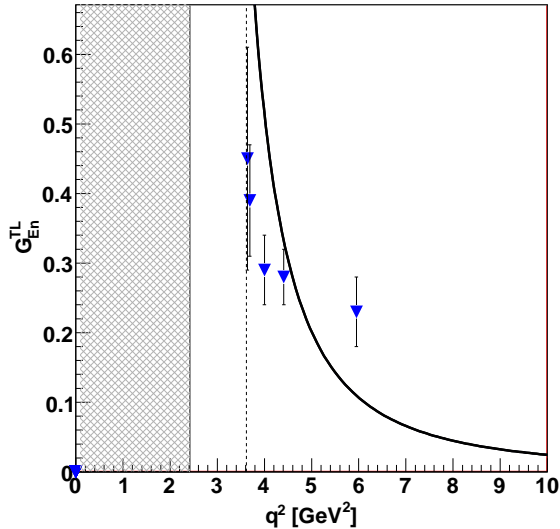


Figure 5. Data on neutron $|G_E| = |G_M|$ FF in TL region, from Ref. [11]. Our prediction for the electric FF is shown as a solid, black line. The solid line indicates the limit where the present model applies. The dashed line indicates the kinematical threshold.

to analytical functions of complex variables, and insures the equality of form factors for large values of $|q^2|$. As form factors are real in the scattering channel, it has for consequence that the imaginary part must vanish in the annihilation channel at large $|q^2|$.

We give also useful and simple parametrizations which reproduce satisfactorily the large q^2 behavior of all nu-

ACKNOWLEDGMENTS

One of us (E.A.K.) acknowledge the hospitality of IPN Orsay where part of this work was done.

* CEA,IRFU,SPhN, Saclay, 91191 Gif-sur-Yvette Cedex, France

- [1] A. I. Akhiezer and M. P. Rekalo, *Sov. Phys. Dokl.* **13** (1968) 572 [*Dokl. Akad. Nauk Ser. Fiz.* **180** (1968) 1081]; *Sov. J. Part. Nucl.* **4** (1974) 277 [*Fiz. Elem. Chast. Atom. Yadra* **4** (1973) 662].
- [2] A. J. R. Puckett et al., *Phys. Rev. Lett.* **104** (2010) 242301 and Refs therein.
- [3] A. I. Vainshtein, V. I. Zakharov, V. A. Novikov and M. A. Shifman, *Sov. J. Part. Nucl.* **13**, 224 (1982) [*Fiz. Elem. Chast. Atom. Yadra* **13**, 542 (1982)].
- [4] V. A. Matveev, R. M. Muradian, and A. N. Tavkhelidze, *Lett. Nuovo Cim.* **7**, (1973) 719.
- [5] S. J. Brodsky and G. R. Farrar, *Phys. Rev. Lett.* **31**, (1973) 1153.
- [6] E. C. Titchmarsh, *Theory of functions*, Oxford University Press, London, 1939.
- [7] R. Baldini, S. Pacetti, A. Zallo, A. Zichichi, *Eur. Phys. J. A* **39**, 315 (2009).
- [8] B. Aubert et al. [BABAR Collaboration], *Phys. Rev. D* **73**, (2006) 012005.
- [9] G. Bardin et al., *Nucl. Phys. B* **411**, (1994) 3.
- [10] M. Ambrogiani et al. [E835 Collaboration], *Phys. Rev. D* **60**, (1999) 032002.
- [11] A. Antonelli et al., *Nucl. Phys. B* **517**, 3 (1998).
- [12] S. Riordan, et al., *arXiv:1008.1738 [nucl-ex]* and Refs. therein.
- [13] L. Andivahis et al., *Phys. Rev. D* **50**, (1994) 5491.